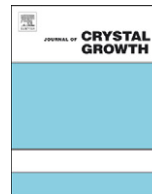




ELSEVIER

Contents lists available at [SciVerse ScienceDirect](http://www.sciencedirect.com)

Journal of Crystal Growth

journal homepage: www.elsevier.com/locate/jcrysgr

Cycloid crystals by topology change

T. Matsuura^{a,b,*}, T. Matsuyama^c, S. Tanda^{a,b}^a Department of Applied Physics, Hokkaido University, Sapporo, Hokkaido 060-8628, Japan^b Center of Education and Research for Topological Science and Technology, Hokkaido University, Sapporo, Hokkaido 060-8628, Japan^c Graduate School of Education, Nara University of Education, Nara 630-8528, Japan

ARTICLE INFO

Article history:

Received 1 August 2012

Received in revised form

19 December 2012

Accepted 25 January 2013

Communicated by Y. Furukawa

Available online 7 February 2013

Keywords:

A1. Crystal morphology

A1. Defects

A2. Single crystal growth

B1. Alloys

ABSTRACT

A cycloid, formerly known as a roulette, is a curve arising from a point on a circumference that rolls on its plane over a fixed straight line, and the cycloid shape is observed in many natural objects formed under a constraint. Here we report the discovery of cycloid-shaped crystals of TaSe₃ obtained via the “topology-change surgery” of thin ring-shaped crystals. We cut the ring-shaped crystals with a focused ion beam. After being cut, they formed a cycloidal shape similar to Cyclotron trajectories of electrons under magnetic and electric fields. We conclude that the inhomogeneous curvature distribution minimizes the bending energy and shear modulation, which corresponds to our shear-less model.

© 2013 Elsevier B.V. All rights reserved.

1. Introduction

The mathematical study of the cycloid (named by Galileo) was very fashionable in the 17th century. Pascal calculated its centre of gravity and its area, Huygens calculated the movement of a material point along a cycloid, and Bernoulli studied a cycloid as a brachistochrone (curve of fastest descent). In nature, the cycloid shapes have been observed, such as the cycloidal patterns on Europa (Jupiter's moon) [1], concave profiles of mountains [2], and topological defect structures in two-dimensional liquid crystals [3], since the cycloid shape is a universal structure derived from Lagrangian calculus of variations under some constraint, namely boundary conditions.

Constraints relate to topology of systems closely, and must change when the topology changes. Thus topology must be a powerful controllable parameter to investigate topological matters in nature, such as a Möbius strip of soap film [4], nanotubes [5] and fullerenes [6], and knots and links of crystals [7–12]. In this paper, we show the cycloid-shaped crystals of TaSe₃, which were obtained by “topology-change surgery” for ring-shaped crystals with diameters of 1–100 μm. We demonstrated to cut the rings with a focused ion beam [13–15], then they opened for relaxation of elastic energy and formed a curve of the cycloid family, namely trochoid curves.

2. Experimental

Ring-shaped crystals, a group of crystals with topologically nontrivial disclinations, such as Möbius strip (π twisted ring), figure-of-8 (2π twisted ring), polyhedral, and Hopf-link crystals, have also been synthesized in MX₃ (M: Ta, Nb, and X: S, Se) systems [7–12]. These crystals have led to new scientific interest in the macroscopic quantum states of charge density waves [13,16–20] and superconductivity [14,21,22] on multi-connected space, and in the problems of interplay between local crystal order and global topology [15,23,24]. While the topological forms of the crystals are similar to nanotubes, their sizes are relatively large (carbon nanotubes are typically of the order of a few nanometers in diameter).

When the ring-shaped crystals are cut, what shape would the crystals become in the open-ring constraint? In the case of thick ring-shaped crystals, the open-ring crystals became arc shape with constant curvatures [15], since the topological defects induced in the ring-shaped crystals homogeneously along the circumferences are dominant. On the other hand, what shape would be realized in the limit of thin thickness? Suppose that a single atomic layer is rolled and becomes a seamless ring. Since the layer is bent and has a finite curvature, the bending energy must be increased. Note that the topology of the ring must be maintained while the bonding energy is lower than the bending energy. If we can cut a single wall carbon nanotube, it becomes a single graphene sheet [25,26], and the curvature becomes zero after cutting to relax the bending energy. Fig. 1(a) shows a schematic diagram of the topology change of single atomic layer

* Corresponding author. Tel.: +81 706 7818.

E-mail address: toru@eng.hokudai.ac.jp (T. Matsuura).

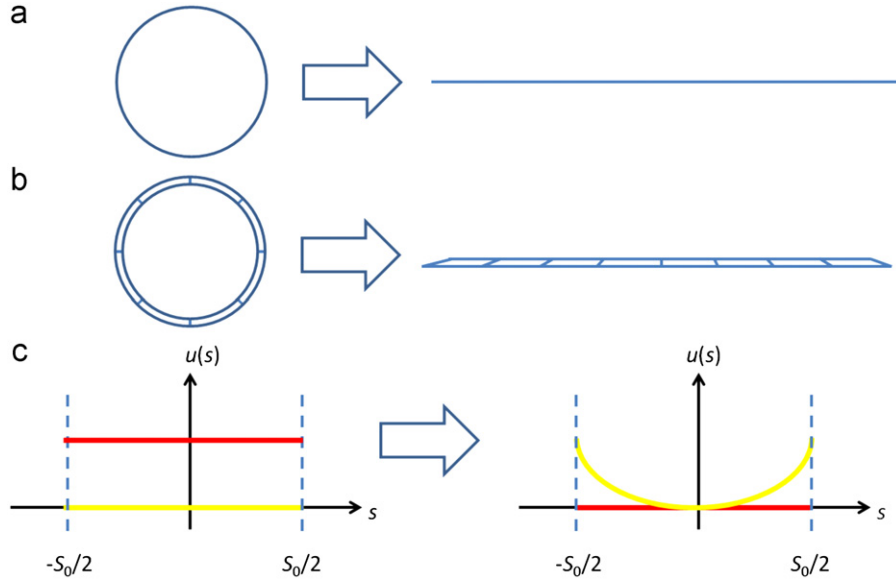


Fig. 1. Schematics of transformation of the ring-rod by topology-change surgery for single-layered ring (a) and double-layered ring (b). (c) Bending energy density (red curve) and shear energy density (yellow curve) for ring-rod [(b) left panel] and the cut-ring [(b) right panel]. $S_0 = 2\pi R$ is the total length of the rod, where R is the initial radius of the ring-rod. (For interpretation of the references to color in this figure caption, the reader is referred to the web version of this article.)

rings. With a rolled double layer, as shown in Fig. 1(b), the interaction between the layers gives the curvature a finite value even after cutting, since the difference of the numbers of atoms in the layers causes shear modulation when the double layer ring is opened. The energy densities of bending and shear for the double layer ring shown in the left and right panels of Fig. 1(b), respectively, are depicted schematically in Fig. 1(c). The closed double layer ring has a homogeneous bending energy density, and there must be no shear modulation. When the ring is forced to be straight, the difference in the number of atoms induces shear modulation. In term of symmetry, the shear magnitude must be zero at the center of the layers, and have its maximum value at the ends. The final form of the multi-layer ring, for example multi-wall carbon nanotubes and thin ring-shaped crystals should be determined by the balance of the shear energy and bending energy.

We propose that the shapes with minimized shear are slipping-cycloid curves, showing an experiment of topology-surgery for thin ring-shaped crystals of TaSe₃. A TaSe₃ crystal has a monoclinic crystal structure with lattice constants $a = 10.402 \text{ \AA}$, $b = 3.495 \text{ \AA}$, $c = 9.829 \text{ \AA}$, and $\beta = 106.26^\circ$ [27] and the circumference of the ring-shaped crystal is parallel to b axis [7,8,15,24]. Using a focused ion beam microfabrication technique, we cut the rings, then found that they opened for relaxation of elastic energy and formed a curve of the cycloid family. We took care to minimize the ion-beam irradiation to whole of the ring-shaped crystals to avoid damage except the cutting parts. Thus the curvatures of the open-rings are dominated by the internal strains induced by the global constraint while crystal growth, and are not a result of modulation induced by the ion-beam irradiation, which have been reported for composite thin layer structures [28].

3. Fitting analysis and discussions

A cycloid curve is the trace of a point on a circle rotating on plain, and is also known as a Brachistochrone curve of mass motion under homogeneous gravity. The cycloid curve can be expanded by one parameter k_s to express a change of curvature from a circle to a straight line, as follows. If a rotating circle with

radius a is slipped, the trace is expressed as

$$x_{\text{out}} = a(k_s\theta + \sin\theta), \quad (1)$$

$$y_{\text{out}} = a(1 - \cos\theta). \quad (2)$$

This curve is known as a trochoid curve, which expresses trajectories of moving electrons in static electric and magnetic fields, and the structure of wave profile for the water surface. The slipping-cycloid (trochoid) curves with various slipping parameters are plotted in Fig. 2(a). When $k_s = 1$, the curve corresponds to a cycloid. For $k_s = 0$, the curve becomes a circle with radius a , and in the limit of $k_s = \infty$, it becomes a straight line. A family of the slipping-cycloid curves, the second layer separated by distance l from the first layer, is expressed as

$$x_{\text{in}} = \left(a - \frac{l}{2}\right)(k'_s\theta' + \sin\theta'), \quad (3)$$

$$y_{\text{in}} = \left(a + \frac{l}{2}\right) - \left(a - \frac{l}{2}\right)\cos\theta'. \quad (4)$$

Here, we must find the relations between k_s and k'_s , and θ and θ' in the condition of minimum shear using Fig. 2(b) and (c). In each figure, the red/blue dotted circle is a circle with a center B/B' rotating with parameter k_s/k'_s . The radius of the blue circle is given by $a' = a - l/2$. The red/blue solid curve corresponds to each slipping-cycloid curve given by the above equations. The line EF in Fig. 2(b) [E'F' in (c)] is the tangent line at D (D'). Line CD (C'D') is perpendicular to EF (E'F'). In other words, C (C') is the crossing point of line AB (AB') and line CD (C'D'). If points C and C' can be on the same point, the shear modulation between two layers is zero when l is sufficiently small. Using this condition ($C = C'$), the relations are given by

$$k'_s = \frac{k_s - \frac{l}{2a}}{1 - \frac{l}{2a}}, \quad (5)$$

$$\theta' = \frac{\theta}{1 - \frac{l}{2ak_s}}. \quad (6)$$

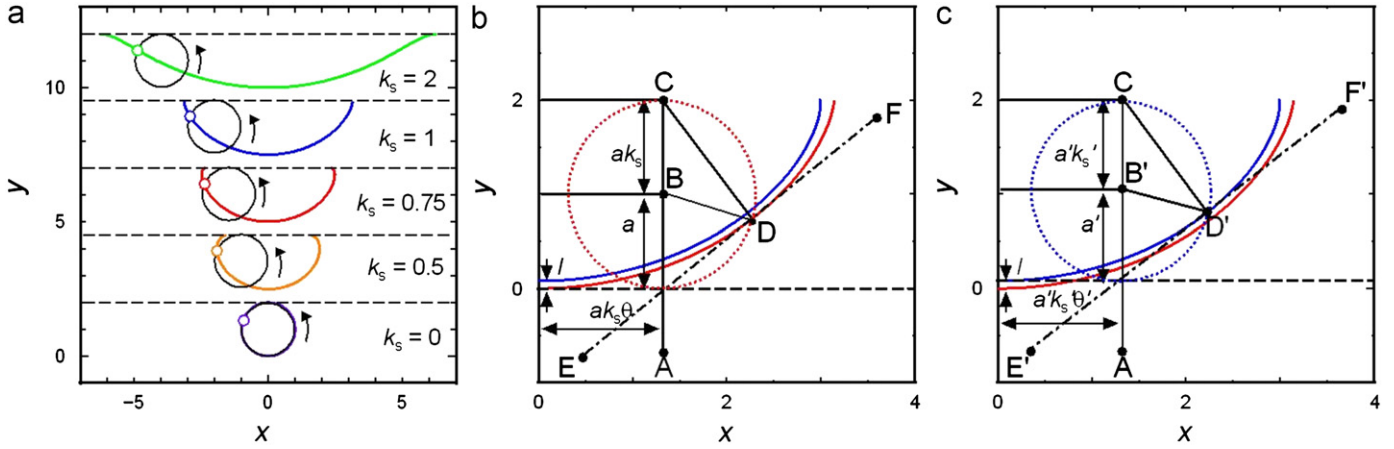


Fig. 2. (a) Slipping-cycloid curves for slipping parameters $k_s = 0, 0.5, 0.75, 1,$ and 2 , respectively. Radius of each rotating circle (a) is set at 1. (b) and (c) drawings of outer and inner layers using the slipping-cycloid curves, respectively. The parameters are described in the text. (For interpretation of the references to color in this figure legend, the reader is referred to the web version of this article.)

Surprisingly only slipping-cycloid curves satisfy the above condition.

To confirm that slipping-cycloid curves exist in nature, we compare the form of thin open-ring crystals in the topology-change surgery experiment [15] with a slipping-cycloid curve (trochoid) and the following natural curves; circle, ellipse, parabola, catenary, hyperbola, and buckling [see Appendix for details of the fitting curves]. If the final form was fitted to a circle (arc), the relaxation of the bending energy was homogeneous. In that case, only the bending energy was associated with the relaxation. If the curvature changed inhomogeneously at the position of the crystal, it meant that the topology-change surgery caused shear modulation.

Fig. 3(a)–(c) is scanning ion beam microscopy (SIM) images of thin ring crystals of TaSe₃ before and after topology-change surgery. Their thicknesses were less than the characteristic thickness τ [15], which means that no cylindrical domain walls were introduced in these ring-shaped crystals. The surgery was performed using a FIB microfabrication technique that was capable of cutting micrometer-size ring-shaped crystals while minimizing any damage. The surgery opened the thin rings and relaxed their bending energy, and their radius of curvature more than double. The coordinate data (x, y) for open-ring crystals were read from the SIM images shown in Fig. 3(a)–(c), and are plotted with open dots in Fig. 3(d)–(f), respectively. Note that each coordinate (x, y) is normalized by the initial radius of each ring-shaped crystal. Fitting analysis was performed while minimizing the average values of $(\Delta x)^2$ [$1/N \sum_N (\Delta x_N)^2$, where Δx_N is the difference between the x coordinate of the N th experimental data and that of each theoretical fitting curve; $\Delta x_N = x_N - x_{\text{fit}}(y_N)$]. The fitting parameters and the average values of $(\Delta x)^2$ are summarized in Table 1.

We found that a trochoid, circle, and ellipse fit the form of the open-rings better than a parabola, catenary, hyperbola, or buckling. The average values of $(\Delta x)^2$ for a trochoid, circle, and ellipse are one order smaller than other curves. We note that this result is consistent with the statement in Ref. [15], where the forms of all open-ring crystals are considered to be circle arcs. An ellipse fits rather than a circle, an ellipse has two fitting parameters. Since a trochoid also has two fitting parameters, k_s and a , an ellipse and trochoid become similar fitting curves. The main difference between trochoid and ellipse can be seen at the ends of the crystals. Shown in the insets of Fig. 3(d)–(f), which focuses on the ends, the trochoid curves fit the experimental data better than the ellipse. These parts are the main difference between a

trochoid and an ellipse. The radius of curvature of a trochoid (for $k_s \leq 1$) becomes small near the ends, and this feature is the same as that of the experimental data. The average values of $(\Delta x)^2$ only at the two ends of the crystals for trochoid curves were obviously smaller than those of an ellipse or a circle. These results indicate that the final form of the open-ring crystals is determined not only by the bending energy, but also by the shear modulation. Since the shear modulation must increase near the ends, thin ring-shaped crystals adopt forms from the slipping-cycloid family to reduce the shear modulation and bending energy.

The shear modulation must be increased when the ring-shaped crystals open. The free length of the crystal axis along the circumference with the inner radius is smaller than that with the outer radius, because the crystal dislocations have been initially introduced into the ring-shaped crystals to reduce the bending energy. After the topology-change surgery, the difference of the free length, however, disturbs relaxation of the bending energy of the crystals. The final curvature must be finite, because of the competition of bending stress and internal bending torque generated from edge dislocations [15]. Thus the strain $\epsilon_x = \epsilon'_x + \epsilon_x^*$, where ϵ'_x is the strain proportional to stress, and ϵ_x^* is the eigen strain associated with plastic deformation. ϵ_x^* represents the dislocation distribution inside the crystals introduced while the crystals were growing due to the global constraint of the ring-shape. To release the bending strain ϵ'_x , the crystals can make shear modulation γ_{xy} via the strain compatibility equation $\partial^2 \epsilon_x / \partial y^2 + \partial^2 \epsilon_y / \partial x^2 - \partial^2 \gamma_{xy} / \partial x \partial y = 0$. Furthermore, the rigidity modulus G of the TaSe₃ crystals must be small because they are bundles of covalently-connected one-dimensional crystal chains with a relatively weak van der Waals force, and the shear modulation could be induced easily.

The distribution of the shear modulation inside the crystals is expected as follows. The strain and stress of the open-rings are symmetric against the center, and the shear modulation is zero at the center, because the shear in the closed-ring before surgery is assumed to be macroscopically zero. After the surgery, the opening crystals have two ends. Due to the boundary conditions, at the ends of the crystals both the stress along the one-dimensional chain and the shear modulation must be zero. Thus the shear modulation could be increased only at the middle of the cut-ring crystals, where the bending energy is more relaxed, and at the ends of crystals, it could not contribute to releasing the bending energy, and the curvature closes to the initial curvature of the ring-shaped crystal before cutting. Therefore, the curves of the cut-ring crystals become the slipping cycloid curves. The curvature distribution

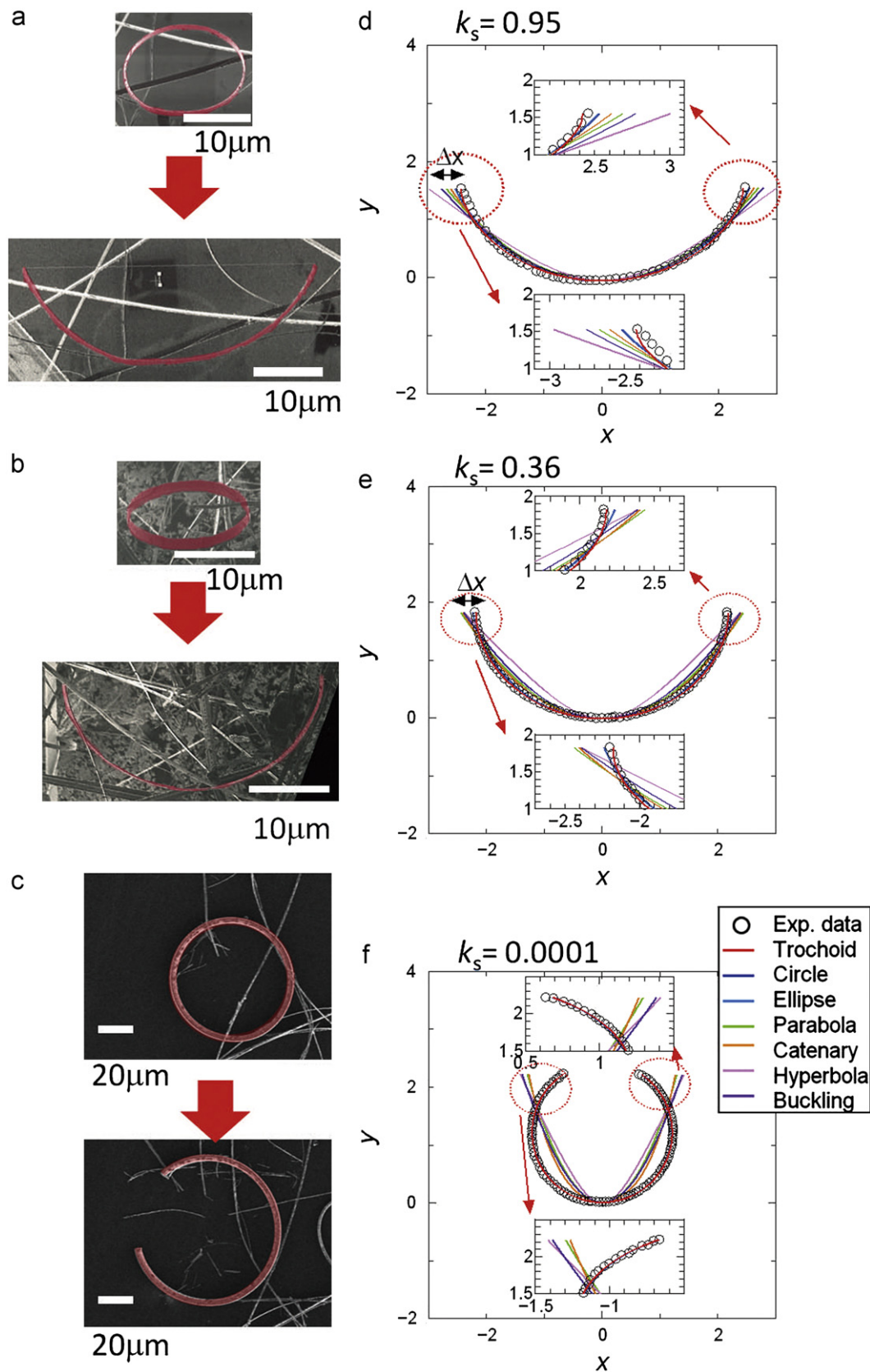


Fig. 3. (a)–(c) Topology-change surgery for two thin ring-shaped crystals. The images were obtained by scanning ion beam microscopy (SIM) with a focused ion beam system. (d)–(f) Final forms of open-ring crystals for (a)–(c), respectively. Coordinates (x, y) , obtained from SIM images (a)–(c), are normalized by the initial radius of each ring-shaped crystal. Trochoid (slipping-cycloid with slipping parameter k_s), circle, ellipse, catenary, parabola, hyperbola, and buckling curves are compared with experimental data. The origin of the coordinates for each fitting curve is $(x, y) = (0, 0)$, and each fitting curve is obtained by minimizing the average values of the squares of the difference of the x direction for all data (Ave. $(\Delta x)^2$).

Table 1

Fitting parameters used for fitting curves in Fig. 3(d), (e) and (f). The average values of the squares of the difference of the x direction for all experimental data (Ave. $(\Delta x)^2$) and that for two ends (Ave. $(\Delta x)^2$ at ends) are displayed.

Fitting curve	Fitting parameter(s)	Ave. $(\Delta x)^2$	Ave. $(\Delta x)^2$ at ends
Trochoid	$k_s = 0.95, a = 0.803$	0.0080	0.0008
Circle	$a = 2.80$	0.0084	0.0087
Ellipse	$a = 2.80, b = 2.82$	0.0084	0.0078
Parabola	$a = 2.12$	0.020	0.060
Catenary	$a = 1.62$	0.011	0.029
Hyperbola	$a = 1.25, b = 1$	0.063	0.31
Buckling	$a = 3.35, b = 5$	0.022	0.11
Trochoid	$k_s = 0.36, a = 1.34$	0.0019	0.0003
Circle	$a = 2.28$	0.0019	0.0035
Ellipse	$a = 2.27, b = 2.23$	0.0018	0.0033
Parabola	$a = 1.80$	0.018	0.068
Catenary	$a = 1.20$	0.028	0.052
Hyperbola	$a = 0.90, b = 1$	0.091	0.044
Buckling	$a = 2.70, b = 5$	0.026	0.045
Trochoid	$k_s = 0.0001, a = 1.21$	0.00048	0.00106
Circle	$a = 1.21$	0.00048	0.00113
Ellipse	$a = 1.2, b = 1.21$	0.00067	0.00085
Parabola	$a = 0.87$	0.090	0.41
Catenary	$a = 0.55$	0.065	0.206
Hyperbola	$a = 0.46, b = 1$	0.132	0.582
Buckling	$a = 1.3, b = 4.3$	0.096	0.536

with the shear modulation is enhanced for thin cut-ring crystals with thinner than about 1 μm , because, for thicker rings than about 1 μm , cylindrical domain walls introduced into the ring and the crystal curvatures are dominated by them [15,24].

4. Summary

In summary, we discussed the final form of thin ring-shaped crystals and proposed the slipping-cycloid model. The model is consistent with a shear-less condition, and describes the form from a ring to a straight line with the slipping parameter k_s . We compared the model curves with the experimental results of topology-change surgery for thin ring-shaped crystals of TaSe₃, and found that the ring-shaped crystals are transformed into slipping-cycloid (trochoid) curves by topology-change surgery. Cycloid crystals realized in superconductors and charge density wave conductors will lead to new electrical transport experiments for quantum brachistochrones [29]. These results also indicate that the conversion of the bending energy and shear modulation plays an important role to determine the global shape of the topological crystals and also topology-change for nanotubes [25,26], and might be a crucial factor of functions with global shape transformation of in micro- and bio-mechanical systems [28].

Acknowledgments

We thank T. Tsuneta, T. Shibayama, K. Yamaya, K. Inagaki, T. Tushima, H. Ohkawa for discussions and supports of experiment. This research was supported by the 21 COE program on Topological Science and Technology of the Ministry of Education, Culture, Sport, Science and Technology of Japan, and the Japan Society for the Promotion of Science.

Appendix A

Circle and ellipse are found in nature. For example, the trajectories of planets rotating around the Sun are ellipse curves.

The coordinates (x,y) of a circle or ellipse passing through $(0,0)$ are expressed as

$$x = a \sin \theta, \quad (7)$$

$$y = b(\cos \theta - 1), \quad (8)$$

where θ is a parameter. When constant a is equal to b , it is a circle. The trajectory of a particle under gravity is a *parabola*, given by

$$y = ax^2. \quad (9)$$

A *catenary* is a curve of the string in homogeneous gravity when its ends are fixed. The coordinates (x,y) of a catenary are described with one constant a , such as

$$y = a(\cosh(x/a) - 1). \quad (10)$$

A *hyperbola* expresses the trajectory of particles with Rutherford scattering, given by

$$x = a \sinh \theta, \quad (11)$$

$$y = b(\cosh \theta - 1). \quad (12)$$

The shape of a long elastic rod applied on a compressing force is called a *buckling* curve. The coordinate of the buckling curve is described with constants a and b , such as

$$y = b \cos(x/a). \quad (13)$$

Using these curves as fitting curves, we compared them with the experimental data for open-ring crystals of TaSe₃.

References

- [1] G.V. Hoppa, B.R. Tufts, R. Greenberg, P.E. Geissler, Formation of cycloidal features on europa, *Science* 285 (1999) 1899–1902.
- [2] B.J. Bridge, G.G. Bridge, Slope profiles of cycloidal form, *Science* 198 (1979) 610–612.
- [3] J.B. Fournier, Curvature elasticity of smectic—a textures with virtual surface singularities, *Physics Review Letters* 70 (1993) 1445–1448.
- [4] R.E. Goldstein, H.K. Moffatt, A.I. Pesci, R.L. Ricca, Soap-film möbius strip changes topology with a twist singularity, *Proceedings of the National Academy of Sciences USA* 107 (2010) 21979–21984.
- [5] S. Iijima, Helical microtubules of graphitic carbon, *Nature* 354 (1991) 56–58.
- [6] H.W. Kroto, J.R. Heath, S.C. O'Brien, R.F. Curl, R.E. Smalley, C₆₀: buckminsterfullerene, *Nature* 318 (1985) 162–163.
- [7] S. Tanda, T. Tsuneta, Y. Okajima, K. Inagaki, K. Yamaya, N. Hatakenaka, A möbius strip of single crystals, *Nature* 417 (2002) 397–398.
- [8] T. Tsuneta, S. Tanda, Formation and growth of NbSe₃ topological crystals, *Journal of Crystal Growth* 264 (2004) 223–231.
- [9] S. Tanda, H. Kawamoto, M. Shiobara, Y. Okajima, K. Yamaya, Ring-shaped crystals of NbSe₃ and TaSe₃, *Journal of Physics IV France* 9 (1999) 379–381.
- [10] S. Tanda, H. Kawamoto, M. Shiobara, Y. Sakai, S. Yasuzuka, Y. Okajima, K. Yamaya, Single crystal rings of NbSe₃: a system for CDW interference, *Physica B* 284 (2000) 1657–1658.
- [11] M. Tsubota, K. Inagaki, T. Matsuura, S. Tanda, Polyhedral topological crystals, *Crystal Growth & Design* 11 (2011) 4789–4793.
- [12] T. Matsuura, M. Yamanaka, N. Hatakenaka, T. Matsuyama, S. Tanda, Topologically linked crystals, *Journal of Crystal Growth* 297 (2006) 157–160.
- [13] T. Matsuura, T. Tsuneta, K. Inagaki, S. Tanda, Topological effect of charge density waves in ring-shaped crystals of NbSe₃, *Physical Review B* 73 (2006) 165118–1–5.
- [14] G. Kumagai, T. Matsuura, K. Ichimura, K. Yamaya, K. Inagaki, S. Tanda, Topological effects of the superconducting vortex state in a TaSe₃ ring crystal: observation of magnetic torque oscillations, *Physical Review B* 81 (2010) 184506–1–4.
- [15] T. Matsuura, T. Tsuneta, G. Kumagai, M. Tsubota, T. Matsuyama, S. Tanda, Topology-change surgery for crystals, *Physical Review B* 83 (2011) 174113–1–5.
- [16] Y. Okajima, H. Kawamoto, M. Shiobara, K. Matsuda, S. Tanda, K. Yamaya, Charge-density-wave sliding in ring-shaped crystals of NbSe₃, *Physica B* 284 (2000) 1659–1660.
- [17] K. Shimatake, Y. Toda, S. Tanda, Quenching of phase coherence in quasi-one-dimensional ring crystals, *Physical Review B* 73 (2006) 153403–1–4.
- [18] T. Nogawa, K. Nemoto, Nonequilibrium relaxation analysis of a quasi-one-dimensional frustrated XY model for charge-density waves in ring-shaped crystals, *Physical Review B* 73 (2006) 184504–1–5.
- [19] T. Matsuura, K. Inagaki, S. Tanda, Evidence of circulating charge density wave current: shapiro interference in NbSe₃ topological crystals, *Physical Review B* 79 (2009) 014304–1–5.

- [20] M. Tsubota, K. Inagaki, T. Matsuura, S. Tanda, Aharonov-Bohm effect in charge-density wave loops with inherent temporal current switching, *Europhysics Letters* 97 (2012) 57011-1-6.
- [21] M. Hayashi, H. Ebisawa, Little-parks oscillation of superconducting möbius strip, *Journal of the Physical Society of Japan* 70 (2001) 3495–3498.
- [22] K. Yakubo, Y. Avishai, D. Cohen, Persistent currents in möbius strips, *Physical Review B* 67 (2003) 125319-1-5.
- [23] M. Hayashi, H. Ebisawa, K. Kuboki, Geometrically frustrated crystals: elastic theory and dislocations, *Europhysics Letters* 76 (2006) 264–270.
- [24] T. Tsuneta, K. Yamamoto, N. Ikeda, Y. Nogami, T. Matsuura, S. Tanda, Relaxation of geometrical frustration in NbSe₃ topological crystals, *Physical Review B* 82 (2010) 014105-1-6.
- [25] D.V. Kosynkin, A.L. Higginbotham, A. Sinitskii, J.R. Lomeda, A. Dimiev, B.K. Price, J.M. Tour, Longitudinal unzipping of carbon nanotubes to form graphene nanoribbons, *Nature* 458 (2009) 872–876.
- [26] L. Jiao, L. Zhang, X. Wang, G. Diankov, H. Dai, Narrow graphene nanoribbons from carbon nanotubes, *Nature* 458 (2009) 877–880.
- [27] E. Bjerkelund, A. Kjekshus, *Acta Chemica Scandinavica* 19 (1965) 701–710.
- [28] K. Chalapat, N. Chekurov, H. Jiang, J. Li, B. Parviz, G.S. Paraoanu, Self-organized origami structures via ion-induced plastic strain, *Advanced Materials* 25 (2013) 91–95.
- [29] A. Carlini, A. Hosoya, T. Koike, Y. Okudaira, Time-optimal quantum evolution, *Physics Review Letters* 96 (2006) 060503-1-4.